

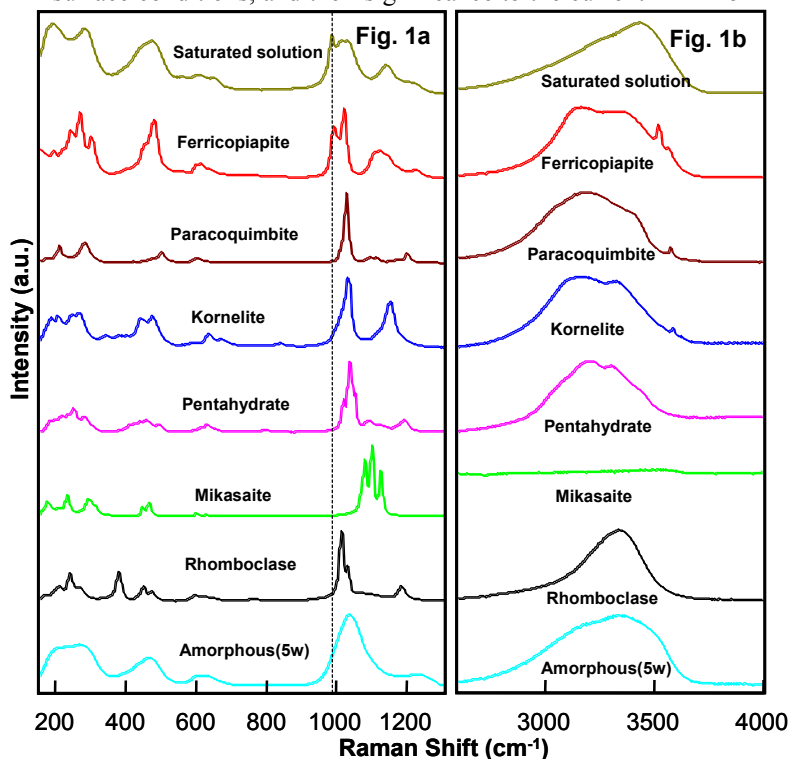
A Systematic Raman, Mid-IR, and Vis-NIR Spectroscopic Study of Ferric Sulfates and Implications for Sulfates on Mars. Zongcheng Ling^{1,2,3}, Alian Wang³, Bradley L. Jolliff³, Raymond E. Arvidson³, H.R. Xia²
¹Department of Space Science and Applied Physics, Shandong University, Weihai, Shandong 264209, China; ²School of Physics and Microelectronics, Shandong University, Jinan, Shandong 250100, China; ³Department of Earth & Planetary Sciences and McDonnell Center for the Space Sciences, Washington University, St. Louis, MO, 63130 (zcling@mail.sdu.edu.cn)

Introduction: Sulfates have been identified on Mars by orbital remote sensing (OMEGA on Mars Express, CRISM on MRO) and during surface exploration (Viking, MER) [1-4]. Orbital observations clearly show evidence for Mg- and Ca-sulfates, but not Fe-sulfates, whereas the MER rovers have found Fe-sulfates at both landing sites. A ferric sulfate (jarosite) was identified with the Mössbauer spectrometer (MB) in Meridiani Planum outcrops (~10 wt.%) [5]. At Gusev Crater, light-toned salty soils were exposed by the wheels of the Spirit rover at various locations within the Columbia Hills [6,7]. These soils are highly enriched in S (up to 35 wt.% SO₃) as seen by APXS [8] and contain ferric sulfates as seen by MB [9]. They are hydrous as seen by MiniTES [10], and could contain ferricopiapite, hydronium jarosite, fibroferrite, rhomboclase and paracoquimbite based on a Pancam spectral analysis [11]. According to mineral mode analyses [6, 12], Mg- and Ca-sulfates coexist with ferric sulfates in the soils. Nevertheless, there are still a large number of unknowns about ferric sulfates on Mars, especially the detailed mineralogy, hydration states, origins, pathways of formation under Mars surface conditions, and their significance to the current

water budget on Mars and their role in Mars' hydrologic history.

To address these unknowns related to ferric sulfates on Mars is the aim of this laboratory spectroscopic study. We prepared seven pure ferric sulfates in the laboratory. Their structures were confirmed by XRD. Their characteristic Raman spectra were then obtained, which form the basis for the next step of this study: to determine stability fields and phase transition pathways of the major ferric sulfates under Mars-relevant environmental conditions. Mid-IR and Vis-NIR spectra were taken on the same samples. This laboratory spectroscopic study is also a preparation for future planetary missions: a Raman-LIBS system will be carried on ESA's ExoMars mission. In addition, the mid-IR, Vis-NIR spectra from well characterized ferric sulfates will aid data interpretation for orbital remote sensing (OMEGA and CRISM) and for surface exploration (e.g., MER Pancam and MiniTES).

Ferric sulfates synthesis: Saturated aqueous solution of ferric sulfate was prepared using Fe₂(SO₄)₃·xH₂O. Rhomboclase (FeH(SO₄)₂·4H₂O) and paracoquimbite (Fe₂(SO₄)₃·9H₂O) were crystallized from mixtures of 0.6g and 0.3g of 98% H₂SO₄ with 4g of saturated aqueous solution, respectively. We produced ferricopiapite (Fe_{4.67}(SO₄)₆(OH)₂·20H₂O) by holding the same saturated solution in a humidity buffer made of KI saturated aqueous solution at 50°C for 3 days. All end products were washed with ethanol to remove the remaining acid in the samples. In addition, we used an amorphous ferric sulfate with five structural waters as the starting material to prepare the other three ferric sulfates. After heating at 200°C in air for 3 days, a pale yellow powder of mikasaite (Fe₂(SO₄)₃) was produced whose structure was confirmed by XRD. When mikasaite was put into a buffer of KI saturated solution at 95°C for one day, it converted to kornelite (Fe₂(SO₄)₃·7H₂O) with a pinkish purple color. When kornelite was put into a buffer of LiCl saturated solution at 95°C for one more day, it changed into a light pinkish phase, which has five structural waters (like the amorphous starting material), but is a crystalline ferric sulfate (Fe₂(SO₄)₃·5H₂O).



XRD and Spectroscopic measurements: A Rigaku Geigerflex X-ray diffractometer

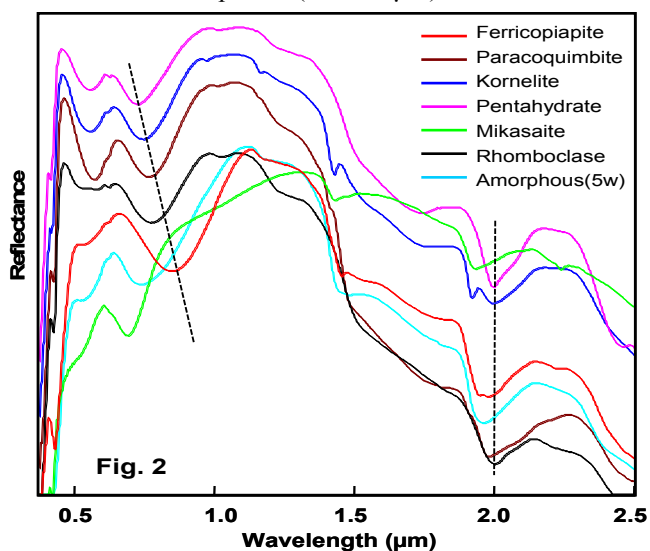
with a $\text{CuK}\alpha$ radiation source was used in this study to confirm the structures of all synthetic ferric sulfates. We used a HoloLab5000-532 laser Raman spectrometer (Kaiser Optical Systems Inc.) to obtain Raman spectra, a Nexus 670 FTIR spectrometer to obtain ATR mid-IR spectra ($4000\text{--}400\text{ cm}^{-1}$) and diffuse reflectance spectra in $1\text{--}5\text{ }\mu\text{m}$ spectral range, and an Analytical Spectral Device to obtain reflectance spectra in $0.4\text{--}2.5\text{ }\mu\text{m}$ spectral range of all synthetic ferric sulfates.

Results: We have confirmed the structures of seven solid ferric sulfates by XRD. Most of the ferric sulfates produced as described above are pure, only paracoquimbite and ferricopiapite contain trace amounts of rhomboclase, which was difficult to exclude during our synthesis procedures.

Figure 1a shows the Raman spectra for seven solid ferric sulfates and a saturated aqueous solution from $150\text{ to }1300\text{ cm}^{-1}$. For each hydrated and anhydrous Fe-sulfate, the symmetric stretching vibrational mode (ν_1) of the SO_4 tetrahedron contributes the strongest Raman peak. As indicated by the dashed line in Figure 1a, the ν_1 peak of different samples shifts from 984 cm^{-1} (for saturated solution) to 1099 cm^{-1} (for mikasaite), following a reduction of the degree of hydration states in these ferric sulfates. The shift of the Raman peak reflects structural variations: more structural or interstitial water molecules will disassociate SO_4 tetrahedra and $\text{FeO}_n(\text{H}_2\text{O})_{6-n}$ octahedra in the crystal framework and decrease the vibrational energy of the SO_4 tetrahedron.

The broad Raman band in the $2600\text{--}4000\text{ cm}^{-1}$ spectral region (Fig. 1b) represents the symmetric stretch mode, the weaker asymmetric stretch mode, and the first overtone of the bending mode of the water molecules in these ferric sulfates. The peak positions and shapes also vary with different crystal structures, thus are diagnostic.

The Vis-NIR spectra ($0.4\text{--}2.5\text{ }\mu\text{m}$) of seven ferric



sulfates are shown in Figure 2. The major spectral variations can be ascribed as follows: (1) In the $500\text{--}700\text{ nm}$ region, the absorption feature due to Fe^{3+} varies from an absorption edge (mikasaite, amorphous, and ferricopiapite) to an absorption band in the spectra of other hydrous phases. In addition, the band width and band depth in the spectra of the latter group gradually reduce and blue-shift following a decrease of the degree of hydration. (2) In the $700\text{--}1000\text{ nm}$ region indicated by a black dashed line in Figure 2, the major absorption band shows a blue shift and becomes narrower for ferric sulfates with lower hydration degree. Notice the spectrum of amorphous ferric sulfates does not follow these two trends. (3) Kornelite shows three prominent diagnostic absorption features at 1428 , 1920 , and 1995 nm . The similar spectral features of ferricopiapite shift to 1454 , 1945 and 1979 nm . The absorption bands of other ferric sulfates in the $1000\text{--}2500\text{ nm}$ range show minor changes in peak positions and in peaks shapes. Further assignments for the peaks in this spectral range will be conducted using the information obtained from Raman and Mid-IR spectra.

Conclusions and future work: We have obtained Raman, mid-IR, Vis-NIR ($0.4\text{--}2.5\text{ }\mu\text{m}$ & $1.0\text{--}5.0\text{ }\mu\text{m}$) spectra from six synthetic crystalline ferric sulfates whose structures were confirmed by XRD, from a pentahydrated amorphous ferric sulfate, and from a saturated aqueous solution of ferric sulfate. As the next step, we are conducting a set of experiments on the stability field and phase transition pathways of five ferric sulfates, using ten humidity buffers at three temperatures. The Raman spectra obtained through this study are used to make non-interruptive, *in-situ* phase identifications through the entire duration of these experiments. The mid-IR and Vis-NIR spectra obtained through this study will be used to better understand the data from orbital remote sensing and surface exploration from Mars.

Acknowledgement: This study is supported by a collaborative project between the Dept. of Space Sciences and Applied Physics at Shandong University and Dept. of Earth and Planetary Sciences at Washington University, and by a Mars Fundamental Research grant NNX07AQ34G. We thank J. Freeman and Paul Carpenter for their help in IR and XRD laboratories.

References: [1] Bibring et al. (2005), *Science*, V307, 1576-1580. [2] Morris et al. (2007) *Seventh International Conference on Mars* #3393. [3] Clark et al. (1982) *JGR*, V87, 10059-10067. [4] Haskin et al. (2005) *Nature*, V436, doi:10.1038. [5] Klingelhöfer et al., *Science*, (2004) V306, 1740-1746. [6] Wang et al. (2006) *JGR*, V111, E02S17. [7] Wang et al. (2007) *Seventh International Conference on Mars* #3348. [8] Gellert et al. (2006) *JGR*, V111, E02S05. [9] Morris et al. (2006) *JGR*, V111, E02S13. [10] Ruff et al., (2006) *JGR*, V111, E12S18. [11] Johnson et al. (2007) *GRL*, V34, L13202. [12] Wang et al. (2006) *JGR*, V111, E02S17. [13] Yen et al. *JGR*, submitted